International Journal of GEOMATE, Nov., 2019 Vol.17, Issue 63, pp. 149 - 156
ISSN: 2186-2982 (P), 2186-2990 (O), Japan, DOI: https://doi.org/10.21660/2019.63.30321
Geotechnique, Construction Materials and Environment

EARTHQUAKE ANALYSIS IN EAST JAVA, INDONESIA BETWEEN 1960 – 2017 USING MARKOV CHAIN MODEL

*Adi Susilo[1], Farizky Hisyam[1] and Wasis[1]

[1]Geophysics Engineering, Brawijaya University, Indonesia

*Corresponding Author, Received: 06 April 2019, Revised: 25 April 2019, Accepted: 15 May 2019

ABSTRACT: Earthquake occurrence in East Java has been analyzed using a Markov Chain Model. The catalog data comprised of earthquake events from East Java and its vicinity from 1960 until 2017. Data were classified into subduction earthquake and inland fault earthquake. After that, the data were declustered using Reasenberg (1985) algorithm for removing the aftershock. Spatial analysis was conducted by dividing the research area into nine regions. Probability transition matrices which give information about the highest probability transition of earthquake occurrence in each region were calculated for different magnitude thresholds. Furthermore, the Chi-Square test was applied to examine the independence between earthquakes occurrence. For seismic hazard analysis purpose, the temporal Markov chain analysis was employed by determining the active (1) and inactive (0) period in each region based on the occurrence of earthquakes with $M \geq 5$ and depth $d < 70$ km. From the two-state probability transition, the mean duration of active and inactive states in each region have been obtained. Both spatial and magnitude analysis results inferred that subduction earthquake with $M \geq 4$, $M \geq 5$, and inland fault earthquake with $M \geq 3$ exhibited strong first-order Markov property, i.e. there was a robust dependency between an earthquake occurrence and the successive occurrence. The mean duration of the inactive state in the research area varied from 2.5 until 13.5 years.

Keywords: Markov Chain, East Java, Earthquake Occurrence, 1960 – 2017, Spatial, Magnitude, Temporal.

1. INTRODUCTION

As an area with the second largest population in Indonesia and traversed by the Sunda arc subduction line, the East Java Province (Figure 1) has a high vulnerability to earthquake hazards. Therefore, it is necessary to conduct earthquake modeling in the East Java region to conduct seismic hazard assessments in the region.

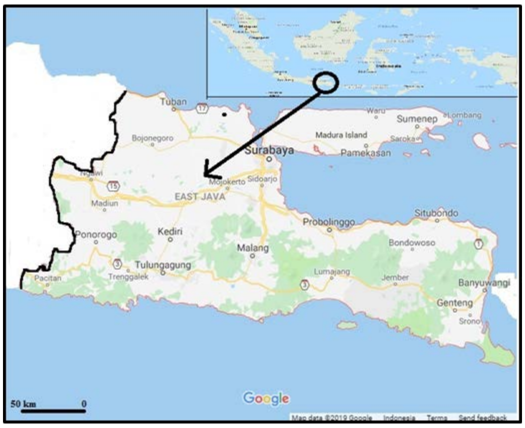

Fig.1. East Java Map

A credible approach to analyzing earthquakes is stochastic modeling [1]. Typically, stochastic modeling is used memoryless [2], i.e., the probability of earthquakes in an area is not affected by previous earthquakes in the region. According to the elastic rebound theory, an earthquake is a moment during the release of accumulated energy from the tectonic force. Thus, the probability of an earthquake in a region is a function of the time and energy accumulated. After a large earthquake occurs, the probability of an earthquake with the same magnitude in the region will immediately drop. Conversely, the probability of a large earthquake happening in an area with no past earthquake will be high [2].

Markov Chain Model is a stochastic model with a one-step memory [3]. This means that future earthquakes in an area are affected by the current earthquake. The Markov Chain Model can determine the future location of earthquakes if the location of the current earthquake is identified. It is increasingly possible as there is an increasing amount of earthquake data available in the earthquake log. The Markov Chain Model has been used in modeling earthquakes in several regions that have high seismic. Some of these include large earthquakes in the Circum Pacific [3], Greece [4], Southern Alaska and the Aleutian Islands [5], Northern Sumatra [6], and the Azores Islands [7]. The research findings can generally explain the sequence of spatial earthquakes in the region.

Markov Chain analysis of the occurrence of large earthquakes in the southern region of Alaska and the Aleutian Islands shows a transition pattern of the occurrence of large earthquake from East to West [5]. In addition, the analysis of shallow earthquake events with Markov chains in the Greek region shows a stress diffusion pattern that is influenced by the local tectonic setting [4]. Furthermore, research on earthquake events in Turkey [8] with the Markov chain shows that earthquake events in the region were investigated in spatial, temporal and magnitude dimensions.

Earthquake events in East Java have been analyzed by a number of previous researchers. Susilo and Adnan (2013) analyzed earthquake events in East Java with Probabilistic Seismic Hazard Analysis (PSHA) [9]. Furthermore, Amalia et al. (2016) conducted an analysis of spatial and temporal earthquake events in East Java with the Gutenberg-Richter distribution [10]. By using Poisson distribution, the study resulted in a recurrence of earthquake events in East Java. However, these studies analyzed earthquake events with memoryless models, which assumed that earthquake events were randomly spatial and temporal and there was no influence between earthquake events and each other. Of course, this is not in accordance with the elastic theory.

Therefore, in this study, an analysis of spatial, magnitude, and temporal earthquakes was carried out in the East Java region using the Markov chain. Spatial analysis is expected to be able to illustrate the area with a high probability of an earthquake. Furthermore, a magnitude of the Markov chain analysis is also performed to determine the probability of an earthquake occurrence of each magnitude after an earthquake with a certain magnitude occurs. Finally, the temporal Markov chain analysis was conducted to determine the average duration of the active and inactive periods of earthquake occurrence with moderate magnitude with shallow depth in the study area.

2. RESEARCH METHOD

The data in this research is earthquake data in East Java and its surrounding from 1960 - 2017. The seismic data is obtained from the United States Geological Survey (USGS). The research area is limited by the coordinates 05º29’24” SL – 11º54’07” SL and 111º00’00” EL – 114º56’32” EL. To avoid confusion in interpretation, the earthquakes in the research location are classified into two, namely earthquakes associated with active fault conditions on land and earthquakes associated with subduction activities.

From the data retrieval process during the predetermined time intervals, the East Java region has 72 inland fault earthquake with $M \geq 3$ and 1,338 subduction with $M \geq 4$. To avoid aftershock in the analyzed data, it is necessary to decluster. In this study, the decluster was based on the Reasenberg algorithm using the program code ZMAP 6 developed by Wyss and Wiemer in 2001. The decluster stage identified 71 inland fault earthquakes and 988 subduction earthquakes. Based on the distribution of the earthquake epicenter, the research location was divided into nine regions. Furthermore, these regions are states of the spatial Markov chain analysis of earthquakes. The whole region can be seen in the Figure 2-3.

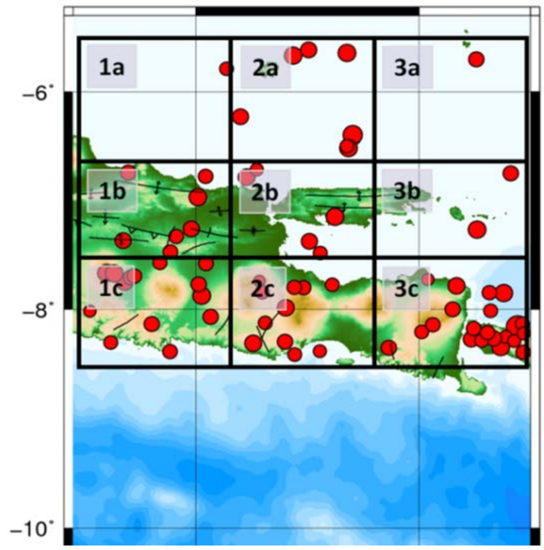

Fig. 2. Seismic map of inland fault earthquake in the research location along with each analyzed region

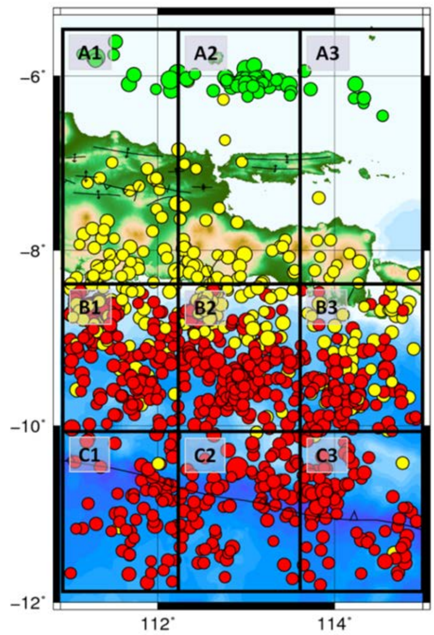

Fig.3. Seismic map of subduction earthquake in the research location along with each analyzed region.

The next step is classifying each major earthquakes in each region based on the location coordinates of the epicenter. Spatial Markov chain analysis is done by compiling a transition frequency matrix. This transition frequency matrix is a size $N \times N$ matrix, where N is the number of conditions or regions used in the study. Thus the obtained matrix measures 9×9 with 81 elements. Each frequency matrix element shows the number of earthquakes transition from region i to region j. Dividing the transition matrix element with the total number of elements in each row will result in the probability transition matrix. The number of matrix elements in each row is 1. The probability transition matrix can help determine the transition with the highest probability if the previous earthquake location is identified. To facilitate the presentation and interpretation of data, the transition diagram can be made from the matrix.

Dividing the number of transition frequencies in each line with a total number of transitions in the research area will result in a vector fixed probability (VPT). VPT can help determine the percentage of earthquakes in each region and compare the observed earthquakes with earthquakes obtained from modeling [4].

Based on the Bayes theorem, the condition is:

$$P_{ij} = Pr\{j|i\} = Pr(j) \quad (1)$$

Thus, the probability of a transition occurring from event i to event j is the probability of occurrence of event j itself. Therefore, all values of the expected probability matrix elements on the same row will have the same value, which is the elements of each row in the VPT. Next, if expthe ectancy transition probability matrix is multiplied by the number of transition frequencies per row, then a transition frequency expectation matrix will be obtained.

In a Markov Chain Modeling, the initial hypothesis assumed that earthquakes in the research location are random and unrelated between the regions. This study used a hypothesis test in the form of a Chi-Squared test. The Chi-Squared test was conducted to determine the relationship between earthquakes in a region and the subsequent earthquakes in other regions. The value of Chi-squared is obtained from the equation:

$$\boldsymbol{x^2} = \sum \frac{(\boldsymbol{O_{ij}} - \boldsymbol{E_{ij}})^2}{\boldsymbol{E_{ij}}} \quad (2)$$

With O_{ij} as the elemen of transition frequency observation matrix and E_{ij} as the elemen of expectancy transition probability matrix.

Next, the value of Chi-Squared is compared with the Chi value of critical squares (table of Chi-squared distribution) with the number of degree of freedom $(N - 1)$ and a significance level of 5%. If the value of the obtained Chi-Squared is smaller than the Chi value of critical squares, the initial hypothesis is accepted. Conversely, if the Chi-Squared value is greater than the critical value, the initial hypothesis is rejected [11] .

Analysis of earthquakes by magnitude is done by classifying earthquake data into three conditions, namely small, moderate, and large earthquakes. In this study there were three earthquake magnitude states :

1. M1 is an earthquake with a magnitude of $4 \leq M < 5$
2. M2 is an earthquake with a magnitude of $5 \leq M < 6$
3. M3 is an earthquake with a magnitude of

Markov chain analysis of geographic events in magnitude is done by making a transition matrix of each situation so that a size 3×3 matrix is obtained. From this matrix, nine transitions of magnitude are obtained. Furthermore, hypothesis testing was carried out using the $M \geq 6$ Chi-Squared test like in spatial analysis.

Temporal analysis of earthquakes is carried out by determining the conditions in each region within a one-year interval from 1960-2017. The analysis shows two states, namely active (1) and inactive (0). An active state (1) of a region is marked with an earthquake magnitude of $M \geq 5$ and depth of d<70km at the time interval analyzed. In contrast, the inactive state (0) is indicated by the interval time with no earthquake of magnitude $M \geq 5$ and a depth of $d < 70km$. The determination of these criteria is based on experience that earthquakes that can be felt and often cause damage are earthquakes with moderate to large magnitudes and with shallow focal depths.

Temporal Markov chain analysis of earthquakes is done by making a transition matrix with conditions 0 and 1 to obtain a size matrix of 2×2 with four possible state transitions that occur, i.e., state 0 becomes 0 (P_{00}), state 0 becomes 1 (P_{01}), state 1 becomes 0 (P_{10})., and state 1 becomes 1 (P_{11}). The probability transition matrix of active or inactive period results in the average active or inactive period duration in each region in units of years using equations $(1/P_{10})$ for the average active state duration and $(1/P_{01})$ for the average inactive state duration

3. RESULT AND DISCUSSION

The calculation results of Chi-Squared values in performing the Markov Chain Modeling for cases of inland fault earthquake for each magnitude limit can be seen in Table 1.

Table 1. N values of Chi-Squared, Chi Critical Squared, and Conclusions for subduction earthquake cases at each magnitude limit.

Magnitude	χ^2	${\chi^2}_{cr}$	Conclusion
$\geq \mathbf{3}$	96,860	83,700	$\boldsymbol{H_0}$ rejected
$\geq \mathbf{4}$	81,968	83,700	$\boldsymbol{H_0}$ accepted
$\geq \mathbf{5}$	21,292	83,700	$\boldsymbol{H_0}$ accepted

Table 1 shows that the initial hypothesis for inland fault earthquake of $\boldsymbol{M} \geq \mathbf{3}$ is rejected while the initial hypothesis for magnitude $\boldsymbol{M} \geq \mathbf{4}$ and $\boldsymbol{M} \geq \mathbf{5}$ is accepted. This implies that inland fault earthquakes of $\boldsymbol{M} \geq \mathbf{3}$ in the research location strongly shows the nature of the first-order Markov chain [4], [11] . Therfore, there is a connection between earthquakes in a region with earthquakes in other regions. In other words, earthquakes are likely not random.

The transition diagram of inland fault earthquake of $\boldsymbol{M} \geq \mathbf{3}$ presented in Figure 4 shows that region 3c is a region in the most visited research area. This means that an earthquake in another region will be followed by an earthquake in the region 3c. This is influenced by the high frequency of earthquakes in region 3c. As an illustration, the VPT value in region 3c is 30%. In addition, the probability of earthquakes transitioning from other regions to region 3c is above 20%. In fact, the inland fault earthquake with the greatest magnitude in the research location occurred in this region, namely the earthquake on July 14, 1976 ($\boldsymbol{M_w}$ **6, 6**).

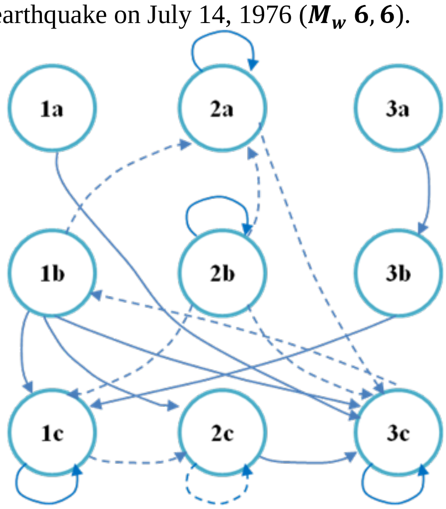

Fig. 4. Transition diagram for Markov spatial Chain Modeling of inland fault earthquake of M≥ 3. The continuous arrow indicates the main transition while the dashed arrow shows the transition with the second highest probability in each region.

The high probability transition in region 3c is due to the active fault in the region, precisely in the area of West Bali and Bali Sea, in the form of a back arc fault[12]. This active fault is the continuation of Flores Fault. It is suspected that this fault continues to East Java (Kendeng Fault) and West Java (Baribis Fault) [13]. Research on strain velocity using GPS in the Java and surrounding areas shows that the largest strain velocity occurs in the West Bali region, which is in the 3c region in this study [13].

In addition to region 3c, other regions that are frequently visited are regions 1c and 2c. This is due to the location of these three regions being in the southern region of the study. The presence of high tectonic and volcanic activity in these regions can trigger an active fault in this region and produce earthquakes. This is also driven by lithology in regions 1c, 2c, and 3c which are generally brittle Quaternary and Tertiary volcanic rocks.

Regions 2a, 2b, 1c, and 3c were observed that another earthquake in a region would follow an earthquake in the same region. This is not due to the impact of aftershocks as the modeled data in this research as the main earthquake data. An explanation of this is the existence of a reactivation process, namely re-activation of a region after an earthquake in the region [4].

The elastic rebound theory further proves its possibility. Earthquakes are cyclical. Rock blocks in the region accumulate energy and are released when an earthquake occurs. Therefore, shortly after the earthquake, energy will decrease. However, with increasing time, energy will accumulate and be rereleased in the future. The time to accumulate this energy is proportional to the magnitude of the earthquake produced. The smaller the earthquake magnitude, the less time is needed to accumulate the energy that can be released to produce an earthquake with that magnitude.

This can also explain the acceptance of the initial hypothesis based on the Chi-Squared test for inland fault earthquake of $\boldsymbol{M} \geq \mathbf{4}$ and $\boldsymbol{M} \geq \mathbf{5}$. This means that earthquakes in the research location are random and independent of each other. Based on the Gutenberg-Richter relation, the frequency of earthquakes is inversely proportional to its magnitude logarithmic. The randomness of this earthquake is due to the lack of data available in the catalog for cases of inland fault earthquakes with large magnitudes. Most inland fault earthquake in the research location have a small magnitude because they are produced from local faults with a relatively short fracture length, whereas the time needed to produce an earthquake with a large magnitude is relatively long, starting from hundreds of years to more. Of course, this time is not covered in the time span analyzed in this study (1970-2017). As an illustration, earthquakes that are categorized as intraplate earthquakes located at the edge of the plate (such as land faults in East Java) have strain velocity of around 0.1 to 10 mm per year and reset time ranging from 100 to 10,000 years [14] .

Earthquake from subduction activity dominates earthquakes in the research location. The resulting earthquake has a fairly large magnitude. Therefore, the magnitude limit used in modeling spatially subducted earthquakes is different from the magnitude limit in modeling inland fault earthquake. The results of the calculation of the Chi-Squared value of subduction earthquake cases for each magnitude limit can be seen in Table 2.

Table 2. N values of Chi-Squared, Chi Critical Squared, and Conclusions for subduction earthquake cases at each magnitude limit.

Magnitude	χ^2	${\chi^2}_{cr}$	Conclusion
≥4	104,594	83,700	$\boldsymbol{H_0}$ rejected
≥5	84,288	83,700	$\boldsymbol{H_0}$ rejected
≥6	25,195	83,700	$\boldsymbol{H_0}$ accepted

Table 2 concludes that the initial hypothesis for subduction earthquakes of magnitude $\boldsymbol{M \geq 4}$ and $\boldsymbol{M \geq 5}$ is rejected while magnitude $\boldsymbol{M \geq 6}$ is accepted. This shows that subducted earthquakes of magnitude $\boldsymbol{M \geq 4}$ and $\boldsymbol{M \geq 5}$ is a strong first order Markov chain. Meanwhile subd,ucti,on earthquakes of magnitude $\boldsymbol{M \geq 6}$ are random. The results of the spatial transition diagram of earthquakes in the research location for subduction earthquake for magnitude $\boldsymbol{M \geq 4}$ and $\boldsymbol{M \geq 5}$ can be seen sequentially in Figures 4 and 5.

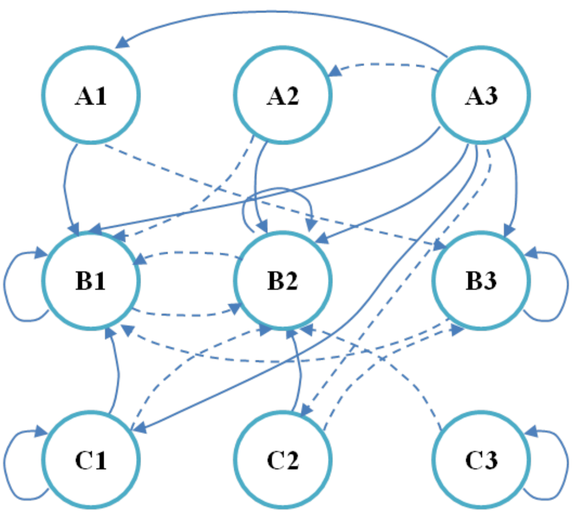

Fig. 5. Transition diagram for spatial Markov chain subduction earthquake modeling of magnitude M≥ 4. Continuous arrows indicate the main transition while the dashed arrow shows the transition with the second highest probability in each region.

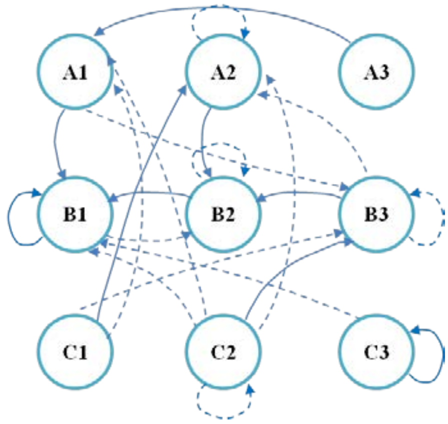

Fig. 6. Transition diagram for spatial Markov chain subduction earthquake modeling of magnitude M≥ 5. The continuous arrow indicates the main transition while the dashed arrow shows the transition with the second highest probability in each region.

Earthquakes that occur in the A1, A2, and A3 regions are earthquakes associated with the Benioff-Wadati zone. Some of them even have a focal depth of up to 600 km. Meanwhile, regions B1, B2, and B3 are earthquakes that occur along the fore arc. Regions C1, C2, and C3 are dominated by megathrust earthquakes or interplate earthquakes associated with the presence of troughs.

The transition diagram in Figures 5 and 6 shows that for earthquakes subduction, region B1 and B2 are the most visited regions. Earthquakes in a region will tend to be followed by earthquakes in regions B1 and B2. The transition to this region is greatly affected by the high seismic activity in region B1, and B2 as both regions are along the seismogenic zone in the East Java region. Seismogenic zones occur when subducting oceanic plates come into contact with lighter continental plates resulting in a friction effect along the contact zone.

The transition diagram shows an interesting pattern where the subduction earthquake in the B3 region will tend to be followed by a similar earthquake in the B2 region while an earthquake in the B1 region will follow the earthquake in the B2 region. In the transition diagram of the subduction earthquake of M≥ 4 magnitude, this transition has the second highest probability. However, in the case of a subduction earthquake of M≥ 5 magnitude, the transition pattern is stronger. The transition pattern may be caused by the different time of energy accumulation in the three regions. When region B1 accumulates energy (no earthquake occurs in region B1) then B2 region releases energy (earthquake occurs in region B2). The possibility of the earthquake energy being released spreads to other regions, triggering the release of energy in the B1 region (an earthquake occurs in the B1 region) while the B2 region again accumulates energy (no earthquake occurs in the B2 region).

Meanwhile, magnitude 6 subduction earthquakes show a random spatial pattern as the East Java region rarely experiences subduction earthquakes with large magnitudes. There are two possible explanations. First, the oceanic plate that subducts in southern East Java is relatively old. Due to its large density, the subduction angle of the plate is also large. This causes the seismogenic zone in East Java to be narrow, producing small magnitudes earthquake. In other words, subduction activities in the East Java region are seismic. The second explanation is that the seismic zone is still locked in southern East Java [15].

Past research has strongly indicated that this is due to seamounts spread on the ground floor of the Indian Ocean [16]. If this seamount is subdued, it can cause the friction field to lock and accumulate large energy. Any time the energy is released can trigger a large earthquake. For example, the largest earthquake case in the research area recorded by the instrument, namely on June 3, 1994 (M_w 7,8) is sourced from the subducted seamount [17].

The analysis results of earthquakes in magnitude with the Markov Chain Model in the research location indicate that from 1973 to 2017, there have been 1,119 large earthquakes or 1,118 transitions with a minimum magnitude limit of M 4. The probability transition matrix obtained from the analysis of the Markov chain is presented in Table 3.

Table 3. Matrix frequency - probability transitions, vector fixed probability, and Chi-Squared value for magnitude states

	M1	M2	M3	VPT
M1	82.4	16.6	1.0	80.4
M2	72.7	26.8	0.5	18.7
M3	70.0	30.0	0.0	0.9

The hypothesis test obtained the Chi-Squared value of 11.134. This value is greater than its critical value with a significance level of 5% and the degree of freedom of 4. In other words, the initial hypothesis is rejected. This indicates that earthquakes in the research location were not randomly generated. If earthquakes with a magnitude of M1, 82.4% happen, the next earthquake to hit will have an M1 magnitude while only 10% of the next earthquakes have a magnitude of M3. Earthquakes with M3 magnitude has a big chance (70%) that a small earthquake M1 magnitude will follow it. As the probability transition value is 0 %, the earthquake with M3 magnitude will not be immediately followed by a magnitude M3 earthquake. This pattern is in line with the elastic rebound theory which states that for a large magnitude earthquake, then the power accumulated is also large. Therefore, it takes a relatively long time to accumulate power and then releases it in the form of a large earthquake. Consequently, the probability of a large earthquake in the same location will be small after an earthquake with the same magnitude hits. On the other hand, areas that have never been hit with a large earthquake will have a significant probability for large earthquakes to hit [3].

The results of temporal analysis of earthquakes with the Markov chain in the research location from 1960 - 2017 are expressed in the two-state probability transition matrix (active and inactive) in Table 4.

Table 4. Probability transition is stated in unit percent.

A1	**0**	**1**	**A2**	**0**	**1**	**A3**	**0**	**1**
0	92.3	7.7	**0**	92.5	7.5	**0**	92.6	7.4
1	66.7	33.3	**1**	80.0	20.0	**1**	100	0

(a)

B1	**0**	**1**	**B2**	**0**	**1**	**B3**	**0**	**1**
0	60.0	40.0	**0**	70.0	30.0	**0**	77.8	22.2
1	88.9	11.1	**1**	66.7	33.3	**1**	76.9	23.1

(b)

C1	**0**	**1**	**C2**	**0**	**1**	**C3**	**0**	**1**
0	88.2	11.8	**0**	83.0	17.0	**0**	68.2	31.8
1	85.7	14.3	**1**	72.7	27.3	**1**	85.7	14.3

(c)

The probability transition values of active to inactive state transitions and inactive to active state transitions in Table 4 respectively show the sequences of active and inactive states in each region as compiled in the histogram in Figure 7. The average duration of each period is stated in years.

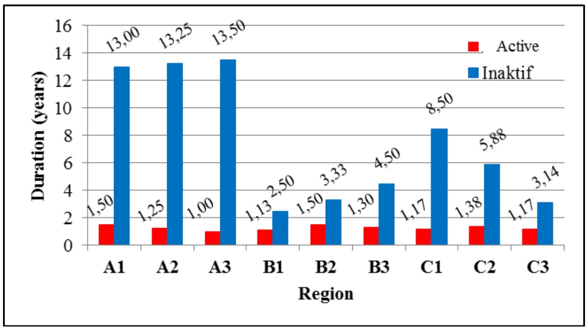

Fig. 7. Average duration (years) of the active and inactive period in each region in the research location.

Temporal analysis earthquakes with Markov chains in the research location indicate a pattern that the area south of East Java has a shorter inactive state average duration than that of the northern part of East Java. The histogram concludes that the A1, A2, and A3 regions have a relatively short duration of the active state, while the duration of the active state is long (≥13 years). On the other hand, regions B1, B2, and B3 have a longer duration of active states (≤1.5 years), and the average duration of the inactive state ranges from 2.5 to 4.5 years. This disparity is caused by the high activity seismicity in the southern region of East Java due to the existence of a subduction zone. Meanwhile, region C1, C2, and C3 have a varied average duration of active and inactive. Region C1 has a short duration of active state (1.17 years) and a long duration of inactive state (8.5 years). Region C1 is a region known as the seismic gap. The inactive period of a region is the period where a region accumulates power to release in the active period.

4. CONCLUSION

The result of the analysis of earthquakes in the East Java region in 1960-2017 with the Markov Chain Model spatially concluded that for subduction earthquakes $M \geq 4$ and $M \geq 5$ and inland fault earthquake $M \geq 3$ in the research location are not random. Subduction earthquake $M \geq 4$ and $M \geq 5$ which occurs in research location will be followed by similar earthquakes in regions B1 and B2 while inland fault earthquake in the research location will be followed by a similar earthquake in region 3c. Subduction earthquakes with $M \geq 6$ and inland fault earthquake with $M \geq 4$ and $M \geq 5$ look random spatially. This is due to the fact that earthquakes are rare in the research area. In general, the highest probability transition of inland fault earthquake occurs in the eastern region in the research location. Meanwhile, subduction earthquakes tend to transition to the west.

Analysis of earthquakes in the magnitude in the research location shows that the large magnitude earthquakes (M3) will be followed by a small magnitude earthquake (M1) with a probability of 70% and followed by a moderate magnitude earthquake (M2) with a probability of 30%, and only 0% followed by large magnitude earthquake (M3). This pattern is due to a long time it takes to accumulate power so that it can be released in the form of a large earthquake.

Temporal analysis of earthquakes results in an average duration of active and inactive states in each region. The relatively long inactivity occurred in the A1, A2, and A3 regions (≤13 years) and short inactive duration were observed in regions B1, B2, B3, and C3 (≤4.5 years).

5. REFERENCES

[1] Mostafei, H., & Kordnoori, S. The Application of the semi-Markov Model in Predicting the Earthquake Occurrence in Alborz Fault Region, Northern Iran. Earth Science India, Vol. 6 (4), 2013, pp.147-159.

[2] Stein, S., & Wysession, M. 2003. An Introduction to Seismology, Earthquakes and Earth Structure (1st ed.). Oxford: Blackwell Publishing.

[3] Patwardhan, A. S. A Semi-Markov Model for Characterizing Recurrence of Great Earthquakes. Bulletin of Seismological Society of America, Vol. 70 (1),1980, pp. 323-347.

[4] Polimenakos, I. C. Shallow Seismic in the Area of Greece: Its Character as Seen by Means of A Stochastic Model. Nonlinear Processes in Geophysics, Vol. 2, 1995, pp. 136-146.

[5] Tsapanos, T. M., & Papadopoulou, A. A. A Discrete Markov Model for Earthquake Occurrences in Southern Alaska and Aleutian Islands. Journal of the Balkan Geophysical Society, Vol.2 (3),1999, pp. 75-83.

[6] Orfanogiannaki, K., Karlis, D., & Papadopoulos, G. A. Identification of Temporal Pattern in the Seismic of Sumatra Using Poisson Hidden Markov Models. Research in Geophysics, Vol. 4 (4969), 2014, pp. 1-6.

[7] Rodriguez, M. C., & Oliveira, C. S. Using Spatial Markovian Chain for the Statistical Analysis of Seismic Occurrences in the Azores Region. Vienna: Natural Hazards and Earth System Sciences, 2016.

[8] Altinok, Y. & Kolcak, D. An Application of the Semi-Markov Model for Earthquake Occurrences in North Anatolia, Turkey. Journal of the Balkan Geophysical Society, Vol. 2, (4), 1999, pp. 90-99.

[9] Susilo, A. & Adnan, Z. Probabilistic Seismic Hazard Analysis of East Java Region, Indonesia. International Journal of Computer and Electrical Engineering, Vol. 5, (3), 2013, pp. 341-344.

[10] Amalia, R. 2016. Studi Variasi Spasial dan Temporal Seismotektonik Jawa Timur. Malang: Jurusan Fisika, FMIPA, Universitas Brawijaya.

[11] Davis, J. C. 1986. Statistics and Data Analysis in Geology (2nd ed.). Toronto: John Wiley & Sons.

[12] Nguyen, N., Griffin, J., Cipta, A., & Cummins, P. R. 2015. Indonesia's Historical Earthquakes: Modelled examples for improving the national hazard map. Canberra: Geoscience Australia.

[13] Koulali, A., McClusky, S., Susilo, S., Leonard, Y., Cummins, P., Tregoning, P., et al. The Kinematics of Crustal Deformation in Java from GPS Observations: Implications for Fault Slip Partitioning. Elsevier (http://dx.doi.org/10.1016/j.epsl.2016.10.039), 2016, pp. 1-11.

[14] Scholz, C. H. 2002. The Mechanics of Earthquakes and Faulting (2nd ed.).

Cambridge: Cambridge University Press.
[15] Newcomb, K. R., & McCann, W. R. Seismic History and Seismotectonics of the Sunda Arc. Journal of Geophysical Research, Vol. 92 (B1), 1987, pp. 421-439.
[16] Bilek, S. L. Influence of subducting topography on earthquake rupture. The Seismogenic Zone of Subduction Thrust Faults, 2007, pp. 123-146.
[17] Abercrombie, R. E., Antolik, M., Felzer, K., & Ekström, G. The 1994 Java Tsunami Earthquake: Slip Over a Subducting Seamount. Journal of Geophysical Research, Vol. 106 (B4), 2001, pp. 6595-6607.